Journal of Electrical and Intelligent Systems (JEIS), Vol. 1, Issue 1
April 2026
ISSN: XXXX-YYYY

Experimental Validation of Enhanced Artificial Rabbit Optimization (ARO)-Based MPPT Method for Photovoltaic Systems Under Partial Shading Conditions

Moh. Zaenal Efendi*, Ircham Badrus Rahmadani, Muhammad Rizani Rusli
Department of Electrical Engineering, Politeknik Elektronika Negeri Surabaya, Indonesia
**Corresponding author: Moh. Zaenal Efendi; email: zenefendi@gmail.com*

Manuscript received 23 March 2026, revised 7 April 2026, accepted 21 April 2026
doi: preprint version.pp1-8

Abstract – *Partial shading often introduces multiple local maxima into the power–voltage (P-V) characteristics of photovoltaic (PV) systems, which makes conventional maximum power point tracking (MPPT) methods prone to converging to suboptimal operating points. To overcome this challenge, this study proposes an Enhanced Artificial Rabbit Optimization (ARO)-based MPPT method by incorporating a time-varying adaptive inertia-weight mechanism, enabling more accurate global maximum power point (GMPP) tracking under nonlinear irradiance conditions. The proposed method was experimentally validated on a laboratory-scale PV platform consisting of three series-connected PV modules, a SEPIC converter, and an STM32-based controller tested under four irradiance patterns. The GMPP reference values were determined through direct experimental P-V scanning. The experimental results indicate that the enhanced method consistently performed better than the conventional ARO baseline, achieving a maximum output power of 98.68 W with a tracking accuracy of 99.93%. Across all test cases, the extracted power and tracking accuracy improved by an average of 1.24% and 1.21%, respectively, without a noticeable increase in tracking time.*

Keywords: *Enhanced Artificial Rabbit Optimization (ARO), Maximum power point tracking, Partial shading, Photovoltaic systems, SEPIC converter*

I. Introduction

Photovoltaic (PV) energy conversion systems are increasingly deployed as part of modern renewable energy infrastructure because of their environmental benefits, modular structure, and ease of installation [1]–[3]. Despite these advantages, the electrical output of PV arrays is highly dependent on the irradiance uniformity and operating temperature [4, 5]. In practical installations, partial shading caused by clouds, nearby structures, trees, or accumulated dust frequently introduces non-uniform irradiance across modules. This condition significantly alters the P–V characteristics and produces multiple local maximum power points, making accurate global maximum power point tracking (GMPP) considerably more difficult [6].

Conventional MPPT techniques, such as perturb and observe (P&O) and incremental conductance (INC), remain widely used because of their simple implementation and low computational burden [7, 8]. A comprehensive review has shown that numerous MPPT methods have been developed over the years, each offering distinct trade-offs between tracking speed, accuracy, and implementation complexity [9]. However, under partial shading, these methods often become trapped around the local maxima because their search process is inherently local. Consequently, the PV system may operate away from the true GMPP, thereby reducing the overall harvested energy.

To overcome this limitation, metaheuristic optimization methods have attracted significant attention because of their strong global search capability in nonlinear operating regions. Algorithms such as particle swarm optimization, genetic algorithms, and other swarm-based techniques have demonstrated improved robustness under partial shading [10]–[12]. In particular, adaptive inertia-weight particle swarm optimization schemes have been introduced to overcome the slow convergence and limited search accuracy of conventional PSO when tracking the GMPP under multi-peak P–V conditions [13]. Among these approaches, the Artificial Rabbit Optimization (ARO) algorithm has recently emerged as a promising bio-inspired method because of its balanced exploration and exploitation mechanism derived from rabbit survival behaviour [11, 12, 14].

Although the conventional ARO method offers strong global search capability, its final approach toward the GMPP may become less precise under severe partial shading, particularly when multiple local peaks are closely

spaced. Under this condition, a well-regulated transition between broad exploration and local refinement becomes critical for accurate MPPT operation. The proposed enhancement is introduced from this perspective and differs from the earlier modified ARO-based MPPT approach, which primarily relied on static parameter mechanisms [15].

Motivated by this practical challenge, this study proposes an Enhanced ARO-based MPPT strategy by introducing a time-varying adaptive inertia-weight term into the original update and selection stages of the ARO framework. The main objective is to improve the final convergence precision while preserving the global search strength of the baseline method. Unlike purely simulation-based studies, the proposed method is validated through hardware implementation using a SEPIC converter and STM32 controller, allowing the observed improvements to be directly linked to realistic PV operating behaviour under controlled partial shading scenarios.

II. System Configuration

A. PV System and SEPIC Converter Configuration

Because the PV output voltage varies with the irradiance and operating conditions, a power-conditioning stage is required to maintain a suitable voltage delivery to the load. Although distributed MPPT topologies based on modular multilevel converters have been proposed to independently regulate each submodule under partial shading conditions [16], such architectures require multiple converters and more complex control. In this study, a SEPIC converter was selected because it can operate in both step-up and step-down modes without changing the output polarity, making it suitable for MPPT applications with varying PV input levels. The complete hardware arrangement of the proposed system, including the PV array, converter, controller, and load interface, is illustrated in Fig. 1.

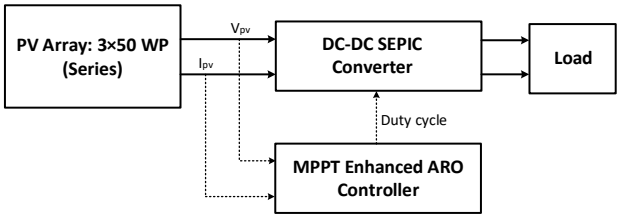

Fig. 1. Block diagram of the proposed MPPT system

In the experimental setup, three 50-Wp monocrystalline PV modules were connected in series to ensure that the array voltage remained within the effective operating range of the SEPIC converter. This arrangement also helped to maintain a stable MPPT operating window when the irradiance changed across the test patterns. The electrical specifications of the PV modules are summarized in Table I.

Because the electrical output of the PV array is highly influenced by environmental conditions, partial shading is an important operating scenario to consider. Partial shading can significantly reduce the efficiency of a PV system owing to discrepancies in the current production among the modules [15, 17].

When shading occurs, the affected cells may function in reverse bias, which can cause hotspots and result in power loss [18]. To counteract these issues, bypass diodes have been installed across the PV modules, as shown in Fig. 2. These diodes alter the I–V and P–V characteristics, resulting in multiple peaks associated with LMPPs and a single GMPP that requires precise tracking using the MPPT algorithm [19], [20].

TABLE I
SPECIFICATION PV MODULE

Parameter	Description	Value	Unit
P_{max}	Max. Power	50	*Watt*
V_{oc}	Open Circuit Voltage	19.3	*Volt*
I_{oc}	Open Circuit Current	2.89	*Ampere*
V_{mpp}	Max. Power Point Voltage	13.83	*Volt*
I_{mpp}	Max. Power Point Current	2.41	*Ampere*
V_{max}	Max System Voltage	1000	*Volt*
Dim	Dimension	725×400×30	*mm*
TC	Test Condition	1000	*Watt/m², at 25°C*

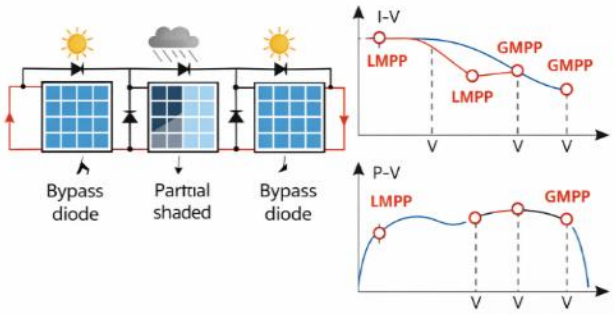

Fig. 2. PV modules with bypass diode

To maintain stable power extraction under these nonlinear PV conditions, a SEPIC converter is employed as the power-conditioning interface. The SEPIC converter regulates the PV output voltage using the PWM control of the switching MOSFET. The circuit of the SEPIC converter is shown in Fig. 3.

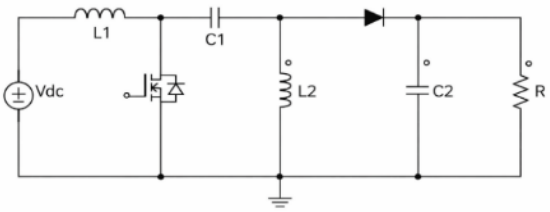

Fig. 3. SEPIC converter circuit

This topology provides a continuous input current and reduces the output ripple, thereby improving the MPPT performance and system stability [21]. Assuming a

converter efficiency of 80%, the component values were determined using Eqs. (1)-(5), as follows:

$$D = \frac{V_o}{V_s + V_o} \tag{1}$$

$$\Delta V_o = 0.1\% \times V_o \tag{2}$$

$$C_1 = C_2 = \frac{V_s \times D}{R \times \Delta V_o \times f} \tag{3}$$

$$\Delta I_L = 20\% \times I_s \tag{4}$$

$$L_1 = L_2 = \frac{V_s \times D}{\Delta I_L \times f} \tag{5}$$

The selected parameters are listed in Table II.

TABLE II
SEPIC CONVERTER PARAMETERS

Parameter	Description	Value	Unit
V_s	Input voltage	41.5	*Volt*
I_s	Input current	2.41	*Ampere*
V_o	Output voltage	14.4	*Volt*
I_o	Output current	5.56	*Ampere*
$C_1 = C_2$	Capacitance	2200	*μF*
$L_1 = L_2$	Inductance	556	*μH*
f	Switching frequency	40	*kHz*
D	Duty cycle	26	*%*

B. An Enhanced ARO-based MPPT Method

The proposed Enhanced ARO-based MPPT method is developed by retaining the original ARO search structure while refining the stages that most strongly influence the final convergence accuracy. In the conventional ARO algorithm, the switching between global exploration and local exploitation is controlled by the energy factor, as shown in Fig. 4. At the beginning of the search, a higher energy factor value A allows the candidate solutions to explore a wider dutycycle region, which helps prevent early convergence to local peaks. As the iterations proceed, the value gradually decreases, such that the search becomes more concentrated around the most promising operating region. This transition mechanism provides a practical balance between search diversity and convergence refinement. However, under severe partial shading, the final transition toward the GMPP region may slightly reduce the tracking precision.

Based on this mechanism, the conventional ARO search process is divided into two stages: global exploration and local exploitation. For clarity, only the core formulations directly related to the proposed enhancement are retained. During exploration, the candidate duty-cycle positions move stochastically across the search space using Eqs. (6)-(11), allowing the algorithm to maintain the solution diversity and avoid premature convergence.

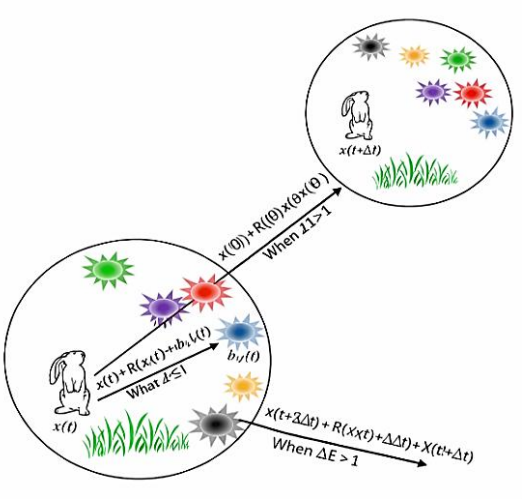

Fig. 4. Search mechanism based on the energy factor *A*

$$v_i^x(t+1) = x_j^x(t) + R \cdot \left(x_i^x(t) - x_j^x(t)\right) + \text{round}\left(0.5 \cdot (0.05 + n_1)\right) \cdot n_1, \quad i, j = 1, \ldots, n \text{ and } j \neq i \tag{6}$$

$$R = L \cdot c \tag{7}$$

$$L = \left(e - e^{\frac{(t-1)^2}{T}}\right) \sin(\pi r_2) \tag{8}$$

$$c(k) = \begin{cases} 1, & \text{if } k = g(l); \quad k = 1, \ldots, d \\ 0, & \text{else } = 1, \ldots, d r_3 \cdot d t \end{cases} \tag{9}$$

$$g = \text{randperm}(d)\,(0,1) \tag{10}$$

$$r_1 \sim \mathcal{N}(0,1) \tag{11}$$

The exploitation stage then narrows the search around the most promising region using the hiding mechanism defined in Eqs. (12)-(18).

$$\vec{b}_{i,j}(t) = \vec{x}_j(t) + H \cdot g \cdot \vec{x}_i(t), \quad i = 1, \ldots, n \text{ and } j = 1, \ldots, d \tag{12}$$

$$H = \frac{T - t + 1}{T} \cdot r_4 \tag{13}$$

$$n_2 \sim \mathcal{N}(0,1) \tag{14}$$

$$g(k) = \begin{cases} 1, & \text{if } k = j; \quad k = 1, \ldots, d \\ 0, & \text{else} \end{cases} \tag{15}$$

$$\vec{v}_i(t+1) = \vec{x}_i(t) + R \cdot \left(r_4 \cdot \vec{b}_{i,r}(t) - \vec{x}_i(t) \right), \quad i = 1, \ldots, n \tag{16}$$

$$g_r(k) = \begin{cases} 1, & \text{if } k = \text{d}r_s \cdot d\text{t}; \quad k = 1, \ldots, d \\ 0, & \text{else} \end{cases} \tag{17}$$

$$\vec{b}_{i,r}(t) = \vec{x}_i(t) + H \cdot g_r \cdot \vec{x}_i(t) \tag{18}$$

The candidate selection process is described in Eq. (19) retains only the better solution obtained at each iteration, while the transition between exploration and exploitation continues to follow the original energy-term definition in Eq. (20).

$$\vec{x}_i(t+1) = \begin{cases} \vec{x}_i(t), & f(\vec{x}_i(t)) \le f(\vec{v}_i(t+1)) \\ \vec{v}_i(t+1), & f(\vec{x}_i(t)) > f(\vec{v}_i(t+1)) \end{cases} \tag{19}$$

$$A(t) = 4\left(1 - \frac{1}{4}\right) \ln \frac{1}{r} \tag{20}$$

The main modification introduced in the proposed method lies in the position update and selection stages, while the original energy factor transition mechanism is preserved. In particular, the update rule in Eq. (16) is replaced by the adaptive form in Eq. (21), where a time-varying inertia weight is used to regulate the influence of the previous duty-cycle position.

$$\vec{v}_i(t+1) = IW(t) \cdot \vec{x}_i(t) + R \cdot \left(r_4 \cdot \vec{b}_{i,r}(t) - IW(t) \cdot \vec{x}_i(t) \right), \quad i = 1, \ldots, n \tag{21}$$

Here, $IW(t)$ denotes the time-varying inertia weight. A larger value in the early iterations encourages a broader exploration of the duty-cycle range, whereas a smaller value in the later stage improves local refinement around the global maximum power point (GMPP).

The updated candidate selection process is expressed by Eq. (22). Using this rule, only candidate positions that provide improved fitness values are retained for the next iteration. In practice, this modification mainly improves the final convergence behavior, allowing the MPPT controller to remain closer to the true GMPP under multi-peak P-V conditions without noticeably affecting the tracking time.

$$\vec{x}_i(t+1) = \begin{cases} IW(t) \cdot \vec{x}_i(t), & f(\vec{x}_i(t)) \le f(\vec{v}_i(t+1)) \\ \vec{v}_i(t+1), & f(\vec{x}_i(t)) > f(\vec{v}_i(t+1)) \end{cases} \tag{22}$$

The overall workflow of the conventional ARO algorithm is illustrated in Fig. 5 as the baseline procedure adopted in this study. In a related but distinct formulation, the modified search mechanism of the Enhanced ARO-based MPPT method is presented in Fig. 6, where several stages are reorganized to accommodate adaptive control requirements.

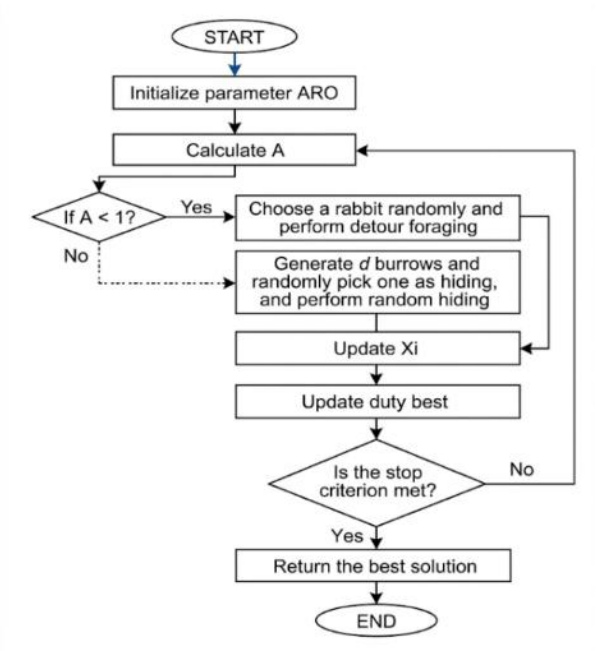

Fig. 5. Flowchart of the ARO

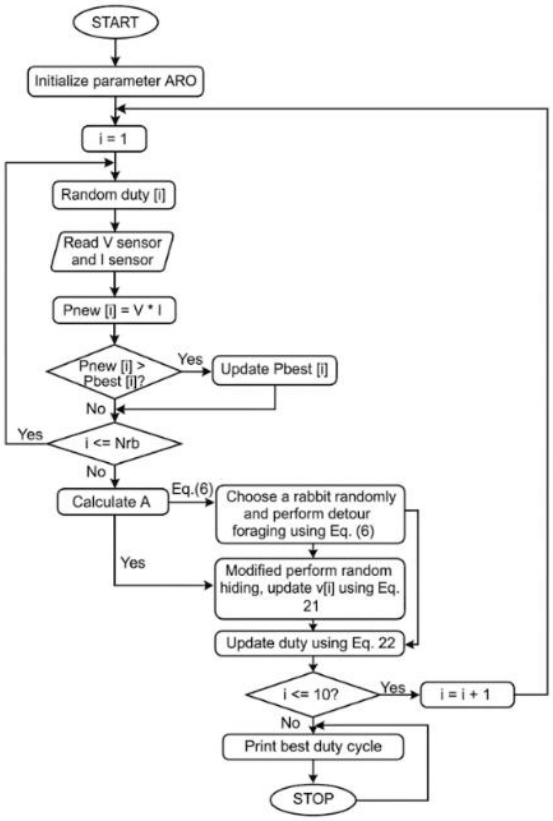

Fig. 6. Flowchart of the Enhanced ARO-based MPPT method

Despite these differences, both approaches share a common structural foundation, including initialization, fitness evaluation, and the exploration–exploitation sequence. The key distinction lies in the incorporation of adaptive update and selection mechanisms in the enhanced method, as defined in Eqs. (21) and (22), which contribute

to improved convergence accuracy under partial shading conditions.

III. Results and Discussion

To evaluate the practical response of the proposed controller, experiments were conducted under four irradiance patterns representing different shading levels. The hardware setup consisted of three series-connected PV modules, a SEPIC converter, and an STM32-based MPPT controller feeding a fixed resistive load, as shown in Fig. 7. All hardware parameters were kept unchanged during the tests, including the converter setting and load condition, so that the performance difference could be directly attributed to the tracking algorithm.

Fig. 7. Experimental prototype of the photovoltaic MPPT system.

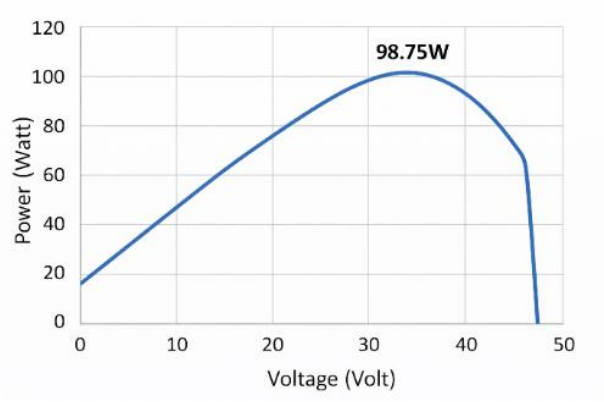

Fig. 8. P-V characteristics of pattern 1 (non shading)

Under Pattern 1 (uniform irradiance), the PV array exhibited a single dominant peak with a GMPP of 98.75 W, as shown in Fig. 8. Both algorithms successfully approached the optimum operating region; however, the Enhanced ARO showed a more accurate trajectory toward the GMPP. This behavior is likely associated with the adaptive inertia-weight term, which moderates abrupt position updates during the final search stage. Experimentally, the proposed method delivered 98.68 W, corresponding to 99.93% tracking accuracy, whereas the conventional ARO reached 97.51 W (98.74%). Although the irradiance condition was relatively simple, the adaptive formulation improved the final convergence precision.

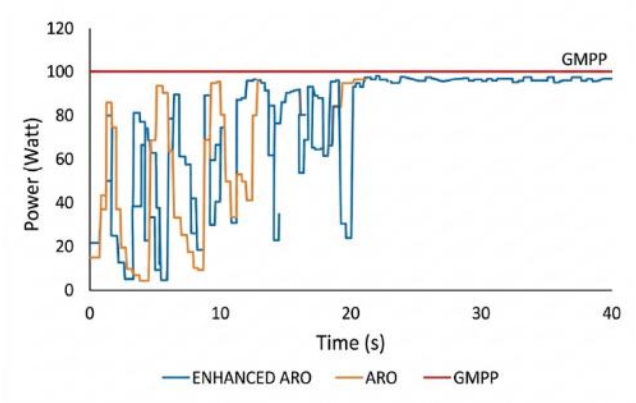

Fig. 9. The experimental results of Enhanced ARO and ARO algorithm pattern 1 (non shading)

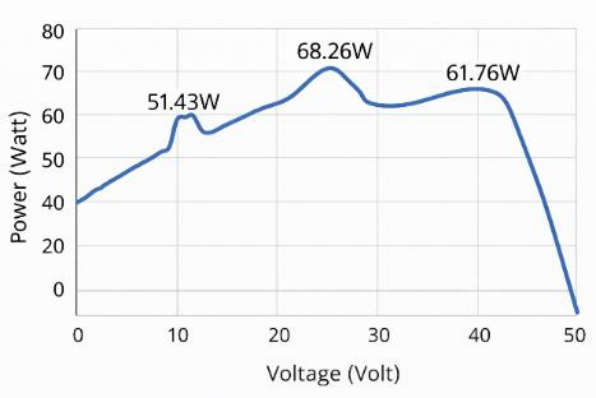

Fig. 10. P-V characteristics of pattern 2 (shading 1)

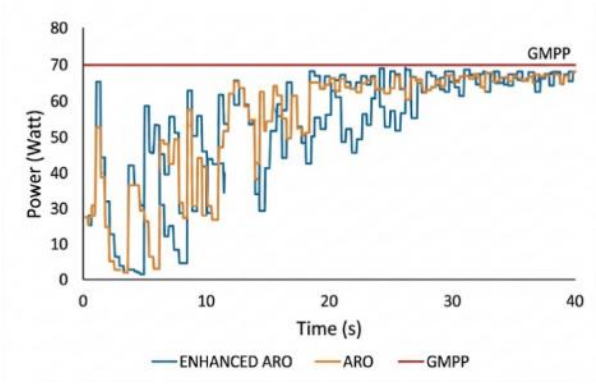

Fig. 11. The experimental results of Enhanced ARO and ARO algorithm pattern 2 (shading 1)

For Pattern 2 (shading 1), the influence of partial shading became more pronounced because the P-V curve contained several local maxima, reducing the GMPP to 68.26 W (Fig. 10). In this condition, the conventional ARO occasionally moved through a suboptimal region

before stabilizing, which is reflected by its slightly lower extracted power. In contrast, the Enhanced ARO preserved a more directed search trajectory toward the global peak, producing 67.94 W with 99.53% accuracy, compared with 67.05 W and 98.23% for ARO. A closer inspection of the transient response suggests that the adaptive weighting mechanism improves the exploration-to-exploitation transition when multiple candidate peaks are present.

A more severe irradiance mismatch was introduced in Pattern 3 (shading 2), where the GMPP decreased to 60.73 W. As shown in Figs. 12 and 13, both algorithms converged faster than in the previous cases because the effective search space became narrower in the dominant power region. However, the Enhanced ARO maintained more consistent tracking accuracy and reached 60.21 W (99.14%), whereas the conventional ARO stabilized at 59.67 W (98.25%). In practical terms, this indicates that the proposed adaptive term remains beneficial even when the power gradient around the GMPP is shallow. The minor fluctuations observed during the first few seconds are mainly attributed to converter transient response and ADC sampling quantization in the STM32 acquisition loop rather than to the optimization logic itself.

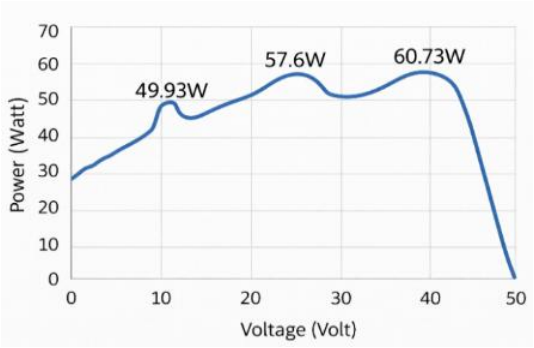

Fig. 12. P-V characteristics of pattern 3 (shading 2)

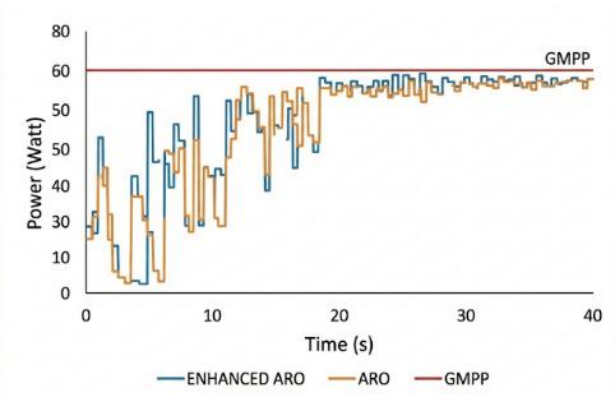

Fig. 13. The experimental results of Enhanced ARO and ARO algorithm pattern 3 (shading 2)

The most nonlinear operating condition was evaluated in Pattern 4 (shading 3), where a strong irradiance mismatch reduced the GMPP to 55.27 W. Under this low-power multipeak condition, accurate GMPP identification becomes more challenging because small duty-cycle deviations can move the operating point toward neighboring local peaks. The Enhanced ARO achieved 54.58 W with 98.75% accuracy, whereas the conventional ARO obtained 53.77 W and 97.29%, as shown in Figs. 14 and 15. The performance gap becomes more visible in this pattern, indicating that the proposed adaptive inertia mechanism is particularly effective when the search landscape is highly non-linear.

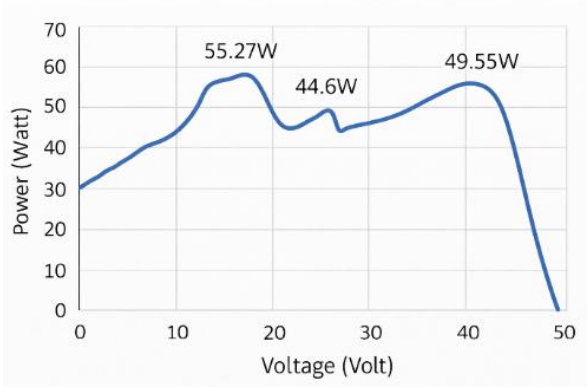

Fig. 14. P-V characteristics of pattern 4 (shading 3)

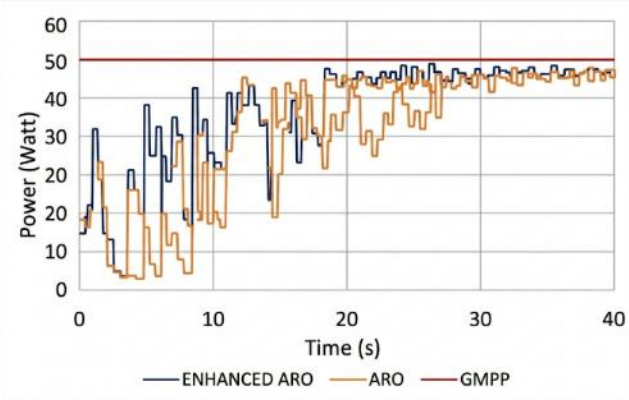

Fig. 15. The experimental results of Enhanced ARO and ARO algorithm pattern 4 (shading 3)

Table III summarizes the overall experimental comparison. Across all irradiance patterns, the Enhanced ARO consistently provided higher extracted power and better tracking accuracy while preserving nearly identical tracking times. The average improvement reached 1.24% in harvested power and 1.21% in tracking accuracy.

From the experimental trend, the main contribution of the proposed enhancement lies in improving the final convergence precision rather than significantly reducing the transient search time.

It should also be noted that the tracking time values in Table III refer to the time required to first enter and remain within the GMPP neighbourhood, whereas the 40 s duration shown in the plots corresponds only to the total observation window for visual comparison. Because both methods used the same population size, iteration number, duty-cycle limits, PWM frequency, and hardware platform, the measured improvement can be directly associated with the adaptive inertia-weight formulation introduced in Eqs. (21) and (22).

TABLE III
EXPERIMENTAL RESULTS PERFORMANCE COMPARISON

Pattern	Algorithm	GMPP (W)	Power Output (W)	Accuracy (%)	Time Tracking (s)
1	Enhanced ARO	98.75	98.68	99.93	20.3
	ARO	98.75	97.51	98.74	20.6
2	Enhanced ARO	68.26	67.94	99.53	20.4
	ARO	68.26	67.05	98.23	20.5
3	Enhanced ARO	60.73	60.21	99.14	18.7
	ARO	60.73	59.67	98.25	18.8
4	Enhanced ARO	55.27	54.58	98.75	18.1
	ARO	55.27	53.77	97.29	18.2

IV. Conclusion

This study experimentally validated the Enhanced Artificial Rabbit Optimization (ARO)-based MPPT method for photovoltaic systems under partial shading conditions. By introducing a time-varying adaptive inertia-weight mechanism into the conventional ARO algorithm, the proposed method improved GMPP tracking performance in terms of extracted power and tracking accuracy while maintaining comparable tracking time. Experimental results from the laboratory-scale SEPIC-based PV platform showed a maximum output power of 98.68 W and a tracking accuracy of 99.93%. Compared with the conventional ARO method, the average improvements reached 1.24% in extracted power and 1.21% in tracking accuracy. These findings indicate that the enhanced ARO method offers better reliability for MPPT under nonlinear shading conditions. The present validation, however, was limited to four representative irradiance patterns on a laboratory-scale setup. Future work should investigate its performance under more dynamic weather variations and real photovoltaic operating conditions.

Conflict of Interest

No Conflict of Interest. The authors declare that they have no conflict of interest regarding the publication of this paper.

References

[1] M. S. Endiz, G. Gökkuş, A. E. Coşgun, & H. Demir, "Review of traditional and advanced MPPT approaches for PV systems under uniformly insolation and partially shaded conditions," Applied Sciences, vol. 15, no. 3, pp. 1031–1031, Feb. 2025. https://doi.org/10.3390/app15031031.

[2] S. Kermadi & J. P. Gaubert, "A comprehensive review of maximum power point tracking algorithms for photovoltaic systems," Renewable and Sustainable Energy Reviews, vol. 90, no. 1, pp. 106188–106188, Jun. 2020. https://doi.org/10.1016/j.rser.2018.10.012.

[3] M. A. B. Siddique, D. Zhao, and A. U. Rehman, "Emerging maximum power point control algorithms for PV system: review, challenges and future trends," Electrical Engineering, 2025, doi:10.1007/s00202-025-03002-0.

[4] J. Kumari & C. S. Babu,"A comprehensive review of maximum power point tracking algorithms for photovoltaic systems under partial shading conditions," Journal of Renewable and Sustainable Energy, vol. 12, no. 6, pp.063703–063703, Nov. 2020. https://doi.org/10.1063/5.0027860.

[5] A. S. Yilmaz & A. Öztürk,"Enhancing the accuracy of MPPT methods for PV systems under rapidly changing environmental conditions," Solar Energy, vol. 180, no. 1, pp. 320–329, Mar. 2019. https://doi.org/10.1016/j.solener.2019.01.034.

[6] N. M. Kumar & K. Sudhakar,"Comparative analysis of MPPT algorithms for photovoltaic system under partial shading conditions," Journal of Electrical Systems and Information Technology, vol. 7, no. 1, pp. 1–16, Jan. 2020. https://doi.org/10.1186/s43067-020-00010-0.

[7] H. Salmi, A. Badri, M. Zegrari, & B. Abdennaceur,"An advanced MPPT based on artificial bee colony algorithm for photovoltaic system under partial shading conditions," International Journal of Power Electronics and Drive Systems, vol. 8, no. 1, pp. 392–401, Mar. 2017. https://doi.org/10.11591/ijpeds.v8.i1.

[8] Y. Lalili, M. Halimi, & T. Bouden, "Optimal MPPT control of a photovoltaic system under non-uniform irradiation," *4th International Conference on Technological Advances in Electrical Engineering (ICTAEE)*, Skikda, Algeria, May 23-34 2023. https://doi.org/10.48550/arXiv.2411.16650.

[9] T. Esram & P. L. Chapman,"Comparison of photovoltaic array maximum power point tracking techniques,"IEEE Transactions on Energy Conversion, vol. 22, no. 2, pp. 439–449, Jun. 2007. https://doi.org/10.1109/TEC.2006.874230.

[10] M. S. Rezk, A. M. Eltamaly, & H. M. Farh,"Global MPPT based on improved metaheuristic optimization techniques under partial shading conditions," Energy Reports, vol. 9, pp. 521–534, 2023. https://doi.org/10.1016/j.egyr.2023.01.045.

[11] L. Wang, Q. Cao, Z. Zhang, S. Mirjalili, & W. Zhao,"Artificial rabbit optimization: A new bio-inspired meta-heuristic algorithm for solving engineering optimization problems," Engineering Applications of Artificial Intelligence, vol. 114, no. 1, pp. 105082–105082, 2022. https://doi.org/10.1016/j.engappai.2022.105082.

[12] Y. Zhang, J. Wang, & X. Li, "Improved multi-strategy artificial rabbit optimization for solving global optimization problems," Scientific Reports, vol. 14, no. 1, pp. 12345–12345, 2024. https://doi.org/10.1038/s41598-024-69010-5.

[13] X. Yuan, D. Yang, & H. Liu,"MPPT of PV system under partial shading condition based on adaptive inertia weight particle swarm optimization algorithm,"in *Proceedings of the IEEE International Conference on Cyber Technology in Automation, Control, and Intelligent Systems*, Shenyang, China, Jun. 2015, pp. 729–733.

[14] R. Kumar & B. Singh, "Advances in artificial rabbit optimization: A comprehensive review," Journal of Computational Intelligence

and Applications, vol. 27, no. 3, pp. 215–240, 2024. https://doi.org/10.1007/s11831-024-10202-7.

[15] G. S. D. Bennet and D. S. Nachimuthu, "Solar PV system with modified artificial rabbit optimization algorithm for MPPT," Electrical Engineering, vol. 106, no. 4, pp. 4543–4559, 2024. doi:10.1007/s00202-023-02231-5.

[16] F. Mohamed, S. Wasti, S. Afshar, P. Macedo, & V. Disfani,"MMC-based distributed maximum power point tracking for photovoltaic systems,"arXiv preprint, Feb. 2020.

[17] A. Mazloumi, A. Poolad, and M. S. Mokhtari, "Optimal Sizing of a Photovoltaic Pumping System Integrated with Water Storage Tank Considering Cost/Reliability Assessment Using Enhanced Artificial Rabbit Optimization: A Case Study," Mathematics, vol. 11, no. 2, p. 463, 2023. https://doi.org/10.3390/math11020463.

[18] N. A. Rahman, M. F. N. Tajuddin, N. M. Mukhtar, & M. Z. Aihsan,"Characterization of photovoltaic module under random partial shading conditions," Journal of Physics: Conference Series, vol. 2312, no. 1, pp. 012031–012031, 2022. https://doi.org/10.1088/1742-6596/2312/1/012031.

[19] H. Ibrahim & N. Anani,"Variation of the performance of a PV panel with the number of bypass diodes and partial shading patterns," in *Proceedings of the 5th International Conference on Power Generation Systems and Renewable Energy Technologies*, Istanbul, Turkey, Aug. 2019, pp. 6–9. doi:10.1109/PGSRET.2019.8882679.

[20] J. C. Teo, R. H. G. Tan, V. H. Mok, V. K. Ramachandaramurthy, & C. Tan,"Impact of partial shading on the P–V characteristics and the maximum power of a photovoltaic string," Energies, vol. 11, no. 7, pp. 1860–1860, Jul. 2018. https://doi.org/10.3390/en11071860.

[21] M. I. Akbar, "SEPIC converter for lead acid battery charger using fuzzy logic type-2 controller," Journal of Electrical Engineering, vol. 6, no. 1, pp. 36–41, Jan. 2022. doi:10.12962/jaree.v6i1.240.

Author Biography

Moh. Zaenal Efendi received his bachelor and master degree in electrical engineering from Institut Teknologi Sepuluh November, Surabaya. He has been with Department of Electrical Engineering, Politeknik Elektronika Negeri Surabaya (PENS), Surabaya since 1993. His researches are interested in power converter technology especially PFC converter, DC-DC converter, Power Electronics for Renewable Energy (MPPT Converter) and inverter. He can be contacted at email: zenefendi@gmail.com.

Ircham Badrus Rahmadani received his degree in Industrial Electrical Engineering from Politeknik Elektronika Negeri Surabaya, Indonesia, in 2025. The applied bachelor's final project involves the design and implementation of a Maximum Power Point Tracking (MPPT) system based on the Modified Artificial Rabbit Optimization (MARO) algorithm for a solar-powered automatic control system. He can be contacted at email: irchambadrus1@gmail.com

Muhammad Rizani Rusli is a lecturer and researcher in Department of Electrical Engineering at Politeknik Elektronika Negeri Surabaya (PENS), Surabaya, Indonesia. He received his bachelor and master degree in electrical engineering from Politeknik Elektronika Negeri Surabaya (PENS), Surabaya. His research interests include Electric Drive, Power Electronics, Control System and Electric Machine. He can be contacted at email: rizani@pens.ac.id